

Carbon export from seaweed forests to deep ocean sinks

Received: 20 April 2023

Accepted: 5 April 2024

Published online: 22 May 2024

 Check for updates

Karen Filbee-Dexter^{1,2}✉, Albert Pessarrodona^{2,3}, Morten F. Pedersen⁴, Thomas Wernberg^{1,2}, Carlos M. Duarte⁵, Jorge Assis^{6,7}, Trine Bekkby⁸, Michael T. Burrows⁹, Daniel F. Carlson^{10,11}, Jean-Pierre Gattuso^{12,13}, Hege Gundersen⁸, Kasper Hancke⁸, Kira A. Krumhansl¹⁴, Tomohiro Kuwae¹⁵, Jack J. Middelburg¹⁶, Pippa J. Moore¹⁷, Ana M. Queirós¹⁸, Dan A. Smale¹⁹, Isabel Sousa-Pinto²⁰, Nobuhiro Suzuki²¹ & Dorte Krause-Jensen²²

The coastal ocean represents an important global carbon sink and is a focus for interventions to mitigate climate change and meet the Paris Agreement targets while supporting biodiversity and other ecosystem functions. However, the fate of the flux of carbon exported from seaweed forests—the world’s largest coastal vegetated ecosystem—is a key unknown in marine carbon budgets. Here we provide national and global estimates for seaweed-derived particulate carbon export below 200 m depth, which totalled 3–4% of the ocean carbon sink capacity. We characterized export using models of seaweed forest extent, production and decomposition, as well as shelf–open ocean water exchange. On average, 15% of seaweed production is estimated to be exported across the continental shelf, which equates to 56 TgC yr⁻¹ (range: 10–170 TgC yr⁻¹). Using modelled sequestration timescales below 200 m depth, we estimated that each year, 4–44 Tg seaweed-derived carbon could be sequestered for 100 years. Determining the full extent of seaweed carbon sequestration remains challenging, but critical to guide efforts to conserve seaweed forests, which are in decline globally. Our estimate does not include shelf burial and dissolved and refractory carbon pathways; still it highlights a relevant potential contribution of seaweed to natural carbon sinks.

The transport of organic carbon from surface waters into the deep ocean is an important mechanism for long-term removal of atmospheric carbon and a key source of energy for mesopelagic and deep-sea ecosystems^{1,2}. Estimates of the processes supporting this flux have focused on export of phytoplankton-derived organic carbon, largely disregarding contributions of benthic primary producers². Seaweed forests (habitats formed by species from the orders Desmarestiales, Fucales, Laminariales and Tilopteridales) assimilate substantial quantities of carbon in the coastal zone by virtue of their exceptional productivity and large spatial extent^{3,4}. Most of this carbon leaves the seaweed forest as either

dissolved organic carbon (DOC)^{5,6} or particulate organic carbon (POC) as detritus⁷. The majority of this POC is exported to nearby habitats due to short residence times of water within seaweed forests (from hours to days^{8,9}) and can subsidize production in other ecosystems¹⁰ or play a role in carbon sequestration if that carbon is locked away for substantial periods (for example >100 years)^{11–13}. Although observations, mass-balance estimates and metagenomic studies suggest widespread export of seaweed carbon to the open ocean and the deep sea^{11,14}, this flux and its ultimate fate are unresolved^{15,16}, such that the contribution of seaweed carbon to the oceanic carbon cycle remains contentious and

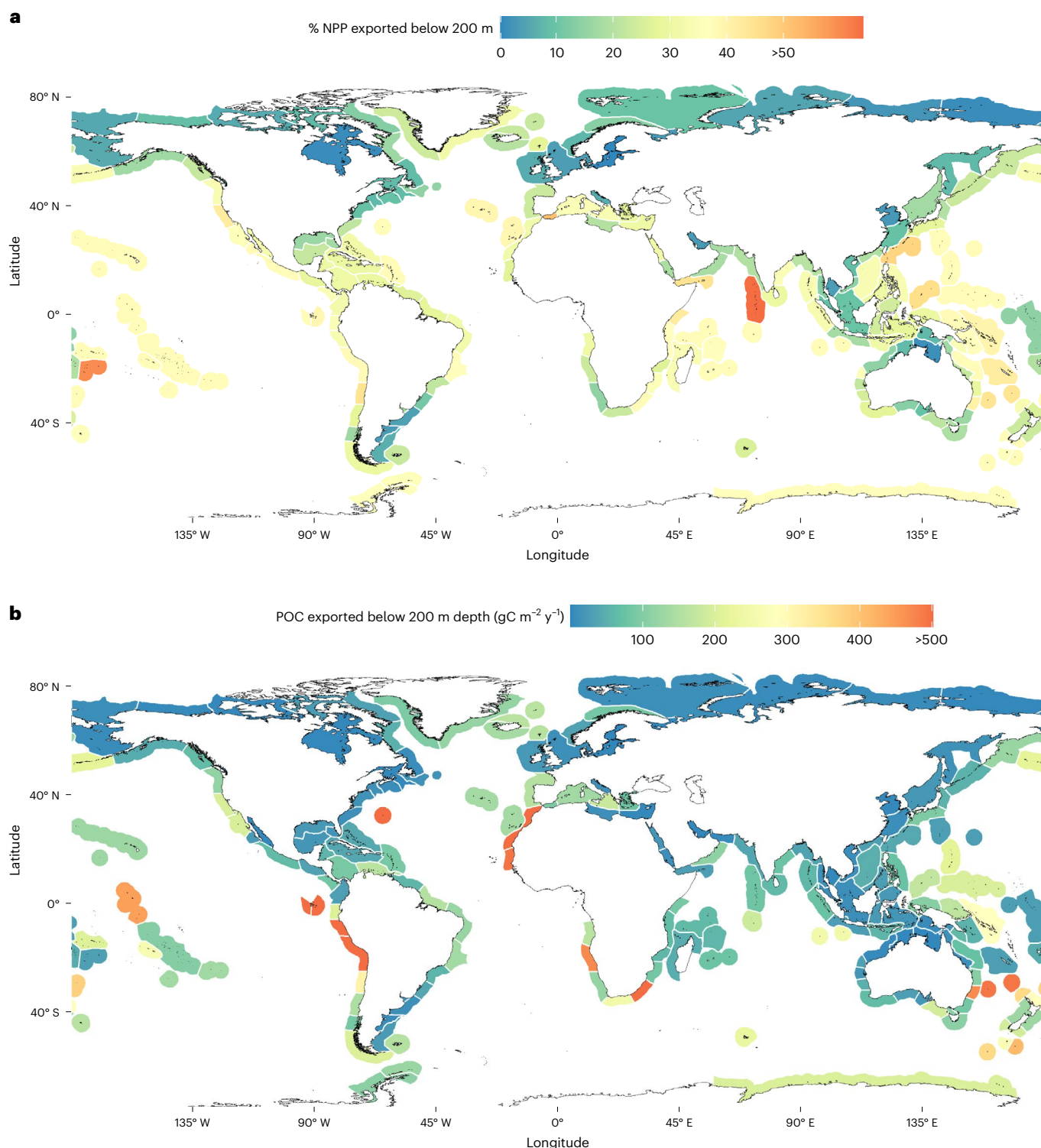


Fig. 1 | Flux of seaweed carbon to deep ocean. a, b, Estimates of the average percentage of seaweed carbon NPP that crosses the world's continental shelves (below 200 m depth) as POC (a) and the average POC per seaweed forest area exported across the shelf (in $\text{gC m}^{-2} \text{yr}^{-1}$) (b) for each ecoregion. Scales are

cropped to 50% and 500 gC m^{-2} to improve visualization of ecoregions with large seaweed areas. All estimates are cropped to the area distribution of the world's seaweed forests³. Map shapefiles are from Natural Earth.

uncertain. A key knowledge gap is the quantity of seaweed-derived carbon that is exported across continental shelves, including the fraction of net primary productivity (NPP) that leaves the upper ocean, and how it varies across coastlines with different geomorphologies¹³. Current estimates of this transport coarsely assume 10% of NPP is exported to the deep ocean as DOC (7.7%) and POC (2.3%)^{11,17}, masking considerable

spatial and temporal variability in these processes^{18,19}. Resolving this variability is crucial for the inclusion of seaweed forests in ocean carbon budgets, national carbon inventories and related opportunities for natural climate change mitigation^{15,20}.

The transport of seaweed POC is determined by local and regional oceanographic processes, the interaction of POC with the seabed and

the rate of POC breakdown and remineralization^{19,21,22}. Seaweed traits such as morphology, buoyancy and reproductive phenology also determine whether seaweeds are transported at the ocean surface, suspended in the water column or as bedload transport along the seafloor²³, with buoyant seaweeds typically being transported farther than non-buoyant ones¹⁹. Approximately 40% of seaweed forest species are negatively buoyant (Supplementary Information) and transported along the seabed. Positively buoyant seaweeds are transported with surface currents but eventually lose their buoyancy or can be entrained in deep waters through vertical mixing due to downwelling, waves or storms, which can rupture gas vesicles due to increased pressure (Supplementary Data 1).

The exchange of water and particles across the shelf break fundamentally underpins the potential for seaweeds to move from the coastal zone to the open ocean, with exchange processes varying strongly over a wide range of spatiotemporal scales^{24,25}. Seaweed POC in coastal or marginal seas or fjords with relatively long residence times may be almost completely remineralized before reaching the shelf break²⁴, apart from refractory components^{26,27} or components that become buried in shelf sediments^{28,29}. Conversely, geomorphic features such as narrow continental shelves or the presence of submarine canyons may facilitate rapid transport of seaweed detritus to the deep sea³⁰. Sequestration of seaweed-derived carbon probably becomes more effective the deeper the seaweed particles reach³¹. Seaweed carbon remineralized within the epipelagic zone typically equilibrates with atmospheric CO₂ within short time spans, whereas most seaweed carbon that reaches the deep sea (>1,000 m) is buried or remineralized and does not exchange with the atmosphere over extended timescales¹¹.

Global transport of seaweed carbon to deep ocean sinks

We estimated the transport of detrital seaweed material from the coastal domain to beyond the shelf break (the 200 m isobath) across the global distribution of brown seaweed of the orders Desmarestiales, Fucales, Laminariales and Tilopteridales (Fig. 1). To do so, we used recent published estimates of global area^{3,32} and production⁴ of brown seaweeds and estimates of the fraction of the production that is exported as detritus (71% ± 6 standard errors (SE)) to obtain a spatially explicit estimate of detritus produced by seaweed forests annually. We combined this information with a 1/8° resolution global model of coastal residence time (CRT), which computed the amount of time a water mass remains within the coastal environment before being exported to the open ocean³³, and measures of seaweed decomposition rates (Extended Data Fig. 1). This yielded an estimate of the fraction of floating and sinking seaweed POC that may be exported to the open ocean before completely decomposing. Differences in the export rates for floating and sinking species were accounted for using experimentally determined water movement thresholds for seaweed bedload transport (0.045 m s⁻¹ ± 0.004 SE), bottom current speeds and estimates of floating longevity (32 days ± 9 SE until buoyancy is lost). Across all exclusive economic zones (EEZs), median CRT was 75 days, with a 25–75% quartile range of 10–441 days. On average, there was no substantial difference between the export of sinking species (14.8% ± 1.9 SE) and that of floating species (13.9% ± 1.1 SE) because most floating seaweeds sank within the continental shelf and entered bedload transport.

Judging from these models, the average export of seaweed detrital POC from subtidal systems to the shelf break was 15 ± 2% of NPP (area weighted mean across 149 EEZs) but was highly variable across the distribution of seaweed forests, ranging from 3% (lower 10%) to 38% (upper 10%) export (Fig. 1a). Variation in export of over two orders in magnitude occurred both within and across national borders and ecoregions (Table 1 and Extended Data Fig. 2). When combined with NPP estimates, we calculated that seaweed forests potentially transport 30 gC m⁻² yr⁻¹ ± 11 SE to deep ocean sinks as POC. Carbon

transport rates ranged from 1 gC m⁻² yr⁻¹ (lower 10%) to 195 gC m⁻² yr⁻¹ (upper 10%) (Fig. 1b). Using estimates of brown seaweed forest extent (1,965,000 km²), this equates to 56 TgC seaweed POC potentially transported beyond 200 m depth every year. This annual rate represents an additional ~1% to the current global estimate of the biological pump (10.2 GtC yr⁻¹ or 1.4–1.7 GtC yr⁻¹ when corrected to 200 m depth³⁴) and 3–4% of the estimated ocean carbon uptake in the global ocean CO₂ sink (2.8 GtC yr⁻¹ or 5–6 GtC yr⁻¹ when corrected to 200 m depth³⁵), both of which ignore coastal contributions. Albeit these estimates are not directly comparable to our estimates of transported seaweed POC as global estimates of the biological pump and ocean CO₂ sink incorporate carbonate and inorganic carbon processes. According to our estimates, countries with the highest potential of seaweed carbon export to the deep ocean include Australia, the United States, New Zealand, Indonesia and Chile (Table 1 and Fig. 2).

Using models of sequestration times for CO₂ injected into the ocean at 200, 530 and 1,000 m depths³¹, we calculated that 15–65% of seaweed detritus remineralized beyond 200 m depth at the shelf break will take >25 years to return to the sea surface, and 6–11% (4–6 TgC yr⁻¹) will take >100 years to return. For seaweeds remineralized beyond 530 m depth, 55–96% of the exported carbon will take >25 years and 23–45% (13–25 TgC yr⁻¹ assuming the total 56 TgC reaches 530 m) will take >100 years to return to the surface. For seaweeds remineralized beyond 1,000 m depth, 36–44 TgC yr⁻¹ will take >100 years to return to the surface (Fig. 3 and Supplementary Data 1). The mean fraction of seaweed carbon remaining at 530 m depth for 100 years was largest for the Arctic (0.5 ± 0.05 SE), Temperate South America (0.3 ± 0.04 SE) and Temperate Northern Pacific (0.3 ± 0.05 SE) realms and the smallest for Temperate Southern Africa (0.1 ± 0.04 SE), Tropical Atlantic (0.1 ± 0.02 SE) and Temperate Australasia (0.2 ± 0.02 SE) realms (Fig. 3 and Supplementary Data 1).

The importance of seaweed in the ocean carbon cycle

The oceanic biological pump—the processes through which inorganic carbon (for example, CO₂) is fixed into organic material by marine photosynthesis and sequestered from the atmosphere through transport into the deep ocean—is generally considered to be driven by phytoplankton³⁶ and migrating fauna³⁷. Although there is a growing appreciation of the potentially large contributions of organic material from vegetated coastal ecosystems to the deep ocean, the transport of this material has not been quantified, representing a critical knowledge gap in the ocean carbon cycle¹¹. In this Article, we show substantial lateral transport of POC from seaweed forests and identify several countries and coastal regions where large quantities of seaweed carbon may be efficiently transferred to the deep ocean, including areas with narrow continental shelves and with strong upwelling supporting high primary production and advective currents. We also find regions where most seaweed carbon is retained within the continental shelf, where there is potential for burial and long-term sequestration^{11,12}. By combining transport estimates with water mass ventilation times, our study provides conservative estimates of seaweed carbon sequestration as it does not include sequestration in coastal sediments or refractory components, which are two additional pathways for long-term removal¹³. Still, the seaweed-derived export of organic carbon to the deep sea represents 1% of the phytoplankton-carbon flux of the biological pump and could form an important component of the exported organic material along some coastal shelf regions. Our global estimate of POC export to deep ocean areas of 56 TgC yr⁻¹ (with a range of 10–170 TgC yr⁻¹) is greater than previous estimates of seaweed POC export to the deep ocean of 35 TgC yr⁻¹ (range 0–85 TgC yr⁻¹)¹¹ and greater than overall carbon sequestration estimates for all other coastal blue carbon ecosystems, increasing the total estimated carbon sequestered by vegetated coastal ecosystems from 88.9 (ref. 38) to 144.9 TgC yr⁻¹. However, not all 56 TgC yr⁻¹ of brown seaweed POC transported beyond the shelf is

Table 1 | National estimates of seaweed carbon export beyond the shelf break

N	Country (EEZ)	Seaweed area (km ²)	NPP (gCyr ⁻¹ m ⁻²)	NPP exported (%)	Exported POC per area (gCy ⁻¹ m ⁻²)	Exported POC total and range (TgCyr ⁻¹)
1	Australia	234,120	196.4	12.4	34.7	5.7 (1.3–26.2)
2	United States	151,521	159.3	16.0	26.1	4.00 (0.39–12.30)
3	New Zealand	24,495	633.8	26.6	157.7	3.90 (0.75–11.40)
4	Indonesia	236,601	110.6	13.0	12.6	3.00 (0.33–10.90)
5	Chile	17,304	551.4	28.9	171.2	3.00 (0.74–7.40)
6	Morocco	3,534	1,340.9	36.3	487.2	1.70 (0.75–4.60)
7	China	159,409	106.2	7.2	10.2	1.60 (0.04–6.70)
8	Peru	2,978	1,512.4	34.7	525.6	1.60 (0.22–3.90)
9	Canada	184,705	93.7	6.0	7.3	1.40 (0.26–4.30)
10	Philippines	25,109	131.3	35.0	52.5	1.30 (0.30–2.70)
11	Nicaragua	19,133	216.3	28.8	66.3	1.30 (0.12–3.30)
12	South Africa	4,782	1,028.1	25.6	259.8	1.20 (0.29–3.60)
13	Bahamas	29,324	93.2	31.7	39.5	1.20 (0.14–2.20)
14	Mexico	34,176	109.3	26.6	33.8	1.20 (0.14–2.80)
15	Spain	5,782	508.9	34.6	194.5	1.10 (0.39–2.80)
16	Japan	26,005	179.8	23.2	42.0	1.10 (0.26–3.20)
17	Russia	148,949	83.4	4.5	7.2	1.10 (0.16–4.00)
18	Brazil	9,201	376.0	26.4	113.9	1.00 (0.14–2.80)
19	Myanmar	40,110	141.3	16.7	24.4	0.98 (0.04–3.50)
20	Greenland	11,007	362.9	18.2	88.9	0.98 (0.28–2.60)
21	Italy	11,418	372.8	19.8	81.6	0.93 (0.35–2.20)
22	Venezuela	7,661	343.3	27.0	110.4	0.85 (0.09–2.20)
23	Panama	5,991	320.7	30.7	132.4	0.79 (0.10–1.60)
24	Mozambique	10,383	215.7	28.7	64.6	0.67 (0.08–1.80)
25	United Kingdom	42,647	280.2	5.4	15.8	0.66 (0–3.00)
26	Norway	20,437	365.9	7.6	32.5	0.66 (0.01–2.80)
27	Iceland	5,538	603.7	20.4	122.6	0.65 (0.07–2.20)
27	Sri Lanka	8,743	177.5	30.7	79.5	0.61 (0.21–1.20)
28	France	16,790	314.0	10.2	33.0	0.55 (0.08–1.90)
29	Bermuda	534	1,241.5	37.6	967.7	0.52 (0.05–0.70)
30	Western Sahara ^a	1,020	1,654.8	33.3	494.7	0.50 (0.23–1.40)
31	Madagascar	10,158	158.6	34.8	47.5	0.48 (0.20–1.40)
33	Vietnam	61,369	70.3	13.1	7.8	0.48 (0.01–1.90)
34	Honduras	9,043	148.8	31.5	52.7	0.48 (0.06–1.20)
35	Portugal	1,674	722.9	36.7	280.9	0.47 (0.17–1.10)
36	Argentina	31,155	282.6	4.8	14.4	0.45 (0.02–1.90)
37	Papua New Guinea	21,760	125.4	28.5	20.1	0.44 (0.13–1.20)
38	Bangladesh	8,608	179.8	25.8	45.9	0.40 (0.03–1.20)
39	Seychelles	5,936	130.8	37.6	63.3	0.38 (0.05–0.60)
40	Falkland Islands ^a	2,668	537.0	22.7	132.5	0.35 (0.06–1.10)
	Other	313,449	0.01–1,443	0.1–66.1	0.01–887	6.5 (1.0–16.9)
	Total	1,965,227		15		56 (10–170)

Seaweed forest area, NPP and potential POC export (TgCyr⁻¹) to deep ocean areas (deeper than 200 m) within EEZ boundaries. Shown are the top 40 EEZs, ordered by POC export. The remaining EEZs are summed under 'Other' and reported in Supplementary Data 1. We estimated that 71% of NPP is available for export from the coastal habitat. Areas are calculated from seaweed distribution models corrected for percentage rocky coastlines. Upper and lower bounds are based on 25% and 75% quartiles for decomposition rates and %NPP available for export. ^aOverlapping claim.

likely to be sequestered as storage capacity is linked to ocean depth (we estimate that ~20 TgC yr⁻¹ of POC reaching 530 m depth is likely to be sequestered). Our estimate underestimates total seaweed POC

export as it does not include brown macroalgae in orders other than Desmarestiales, Fucales, Laminariales and Tilopteridales, or green or red macroalgae, which have extensive global distributions and

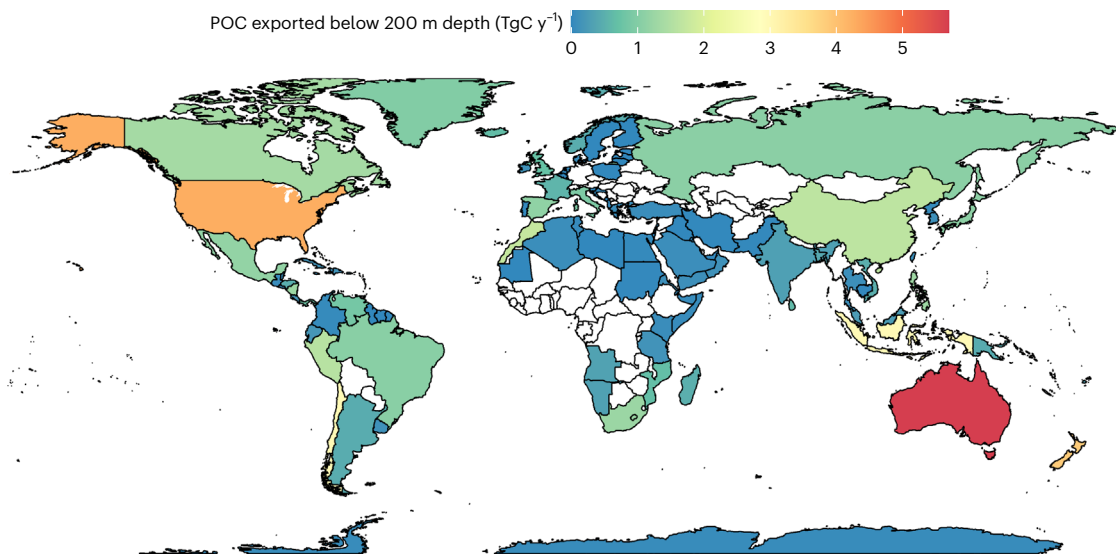


Fig. 2 | National estimates of seaweed carbon export. Annual potential export of seaweed-derived POC (TgC yr^{-1} (or million tonnes yr^{-1})) below 200 m depth within EEZ boundaries. Map shapefiles are from Natural Earth.

considerable rates of total NPP, albeit are less studied compared with seaweed forests³. However, the estimated annual NPP of brown seaweed forests used in the calculations represents an upper limit as it assumes such forests are present on all rocky seafloor within their distribution (Supplementary Information).

Creating national estimates of seaweed carbon drawdown and potential sequestration

Our study suggests that on average, 15% of the annual production of seaweed forests may cross the continental shelf and reach deep ocean water masses, which when accounting for geographic differences in NPP equates to 18% of the 317 TgC yr^{-1} global seaweed forest NPP (Supplementary Data 1). Once seaweed material enters these deeper regions, it can be rapidly decomposed, used by fauna³⁹ or buried, but a portion of the material can remain effectively sequestered for decades to centuries due to the characteristic long ventilation times of deep-water masses. These estimated sequestration timescales at 200 and 1,000 m depths probably represent lower and upper thresholds for the fate of seaweed POC, as a portion that crosses the 200 m shelf break is assumed to continue to sink and/or be transported along the seafloor to deeper regions as it remineralizes. Hence, many deep ocean areas near coastal zones provide suitable long-term carbon sinks³¹ within the centenary timescales relevant for climate change mitigation.

Our calculations provide national-level estimates of brown seaweed area, NPP and POC export below 200 m depth, which may eventually be required for seaweed forests to be incorporated into national strategies for ocean carbon accounting frameworks and mitigation policies, as well as Nationally Determined Contributions under the Paris Agreement^{13,20}. Yet our results also highlight high spatial variation in transport potential and sequestration timescales across ecoregions and ecological realms. This variation should be further resolved with fine-scale models and incorporated into regional assessments of the effectiveness of seaweed-based climate mitigation strategies^{15,19}, and used to verify the permanence of seaweed carbon that reaches the deep ocean.

The majority (~82%) of seaweed POC was not exported beyond the 200 m isobath and was, therefore, retained within the continental shelf. There it can enter coastal food webs and may represent an important trophic subsidy to less productive habitats⁷, be buried in coastal sediments or be remineralized with a potential return of CO_2 to the atmosphere. Seaweed depositing on the continental shelf will

contribute to carbon sequestration only when buried in sediments²⁸ or if it is refractory. Long-term organic carbon burial on the continental shelf is governed by the efficiency of vertical delivery versus lateral fluxes, sediment accumulation rate, bioturbation, natural and human-induced resuspension and the efficiency of organic matter degradation⁴⁰. Burial rates may be enhanced in areas such as fjords and other accreting coastal blue carbon habitats such as seagrass and mangroves^{41,42} or in sediments close to sources of seaweed POC^{12,29}. Studies tracing seaweed detritus in cores on the continental shelf are very limited, yet seaweed carbon has been found in all layers of shelf sediments, including those deposited 120 years ago²⁹, suggesting potential for long-term storage in some locations. Better knowledge of post-depositional processes in shelf sediments, and the impacts of disturbance (for example, trawling, infrastructure) on natural carbon storage, is required to determine the fate of seaweed-derived carbon and sequestration rates on these continental shelves.

Our calculations do not include exported seaweed DOC, which is a potentially important pathway to remove carbon from short-term cycles—with sequestered DOC probably representing a key mechanism for export of seaweed carbon^{11,43}, a (unknown) proportion of which may be recalcitrant and not amenable to fast remineralization^{44,45}. Although the coast–ocean water exchange approach used here would be a good approximation for offshore DOC transport¹¹, it cannot be used to determine the depth DOC reaches. Seaweed DOC degradation estimates are also too few, measured on too short timescales and methodologically inconsistent to make spatially meaningful estimates of the amount remaining for transport over time¹³. Resolving this missing flux should therefore be a priority for future research. Still, evidence from a few locations suggests that substantial amounts of seaweed DOC are exported to coastal waters beyond seaweed habitats^{5,43}, a fraction of which may persist as a refractory component that will undergo slow decomposition over years to centuries^{13,44}. In addition to DOC, evidence suggests that a significant portion of seaweed POC is refractory²⁷, but variable depending on species and environmental conditions, and its permanence is challenging to trace and verify for long timescales¹³. According to our estimate of global seaweed NPP of 317 TgC yr^{-1} , for each 1% of seaweed carbon that is refractory, there is an additional 3 TgC yr^{-1} removed from short-term carbon cycles on the continental shelf.

Further refinement of our estimates of export rates and sequestration timescales will require high-resolution hydrographic models

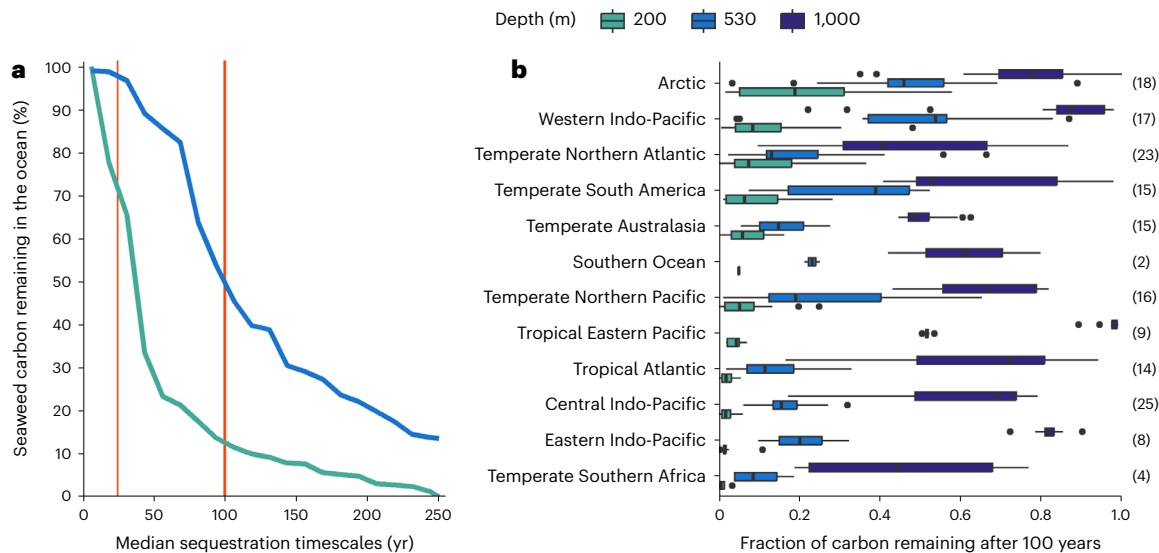


Fig. 3 | Sequestration timescales for exported seaweed carbon. **a**, Cumulative seaweed carbon exported beyond the continental shelf break with a range of sequestration timescales. Calculations are based on modelled global estimates of CO₂ leakage rates³¹ at 200 m (green) and 530 m (blue) depths, cropped to the distribution of seaweed forests. Estimated sequestration timescales for each ecoregion were combined with estimates of seaweed carbon export for each ecoregion and summed to determine cumulative export. Vertical lines show 25 and 100 year timescales. **b**, Fraction of discharged carbon remaining at

200 m, 530 m and 1,000 m depths off coastal ecoregions containing seaweed forests ($n = 188$; Supplementary Data 1), calculated from global models of the sequestration fraction of injected CO₂ with depth³¹ and summarized for each ecological realm by box plots showing the median and 25th and 75th percentiles, whiskers showing 1.5 times the inter-quartile range and text in brackets showing the number of ecoregions in each realm. Realms are ordered by median fraction of CO₂ remaining at 500 m depth for 100 years.

for the coastal zone and open ocean (Supplementary Information). However, our estimates largely agree with regional seaweed particle tracking models forced with higher-resolution ocean current data²¹. For example, in mid Norway, less than 5% of all seaweed particles released along the coast crossed the 200 m isobath²¹, which is similar to our estimates of 8% (± 5 s.d.) for the Southern Norway ecoregion. In Greenland, less than 20% of drifting macroalgae released in an inner fjord were exported beyond the mouth of the fjord¹⁸, suggesting only slightly lower export compared with our estimate of 24% ± 15 s.d. in West Greenland ecoregion. In Western Australia, 17–29% of seaweed carbon crossed the 200 m depth contour off the Houtman ecoregion⁴⁶, which is similar to our estimates of 25% (± 11 s.d.).

Overall, we provide a high-level estimate supporting the conclusion that substantial amounts of seaweed-derived organic material could enter the deep ocean annually. These pathways of seaweed carbon flow should be included in future models of the ocean carbon cycle. Our estimates provide an important first step towards understanding the role brown seaweed forests play in carbon sequestration, which need to be supplemented with estimates of DOC fluxes and shelf burial^{13,28,43}, as well as fluxes of CO₂ and other greenhouse gases between seaweed forests¹⁵ and other seaweed ecosystems and the atmosphere¹⁵. Seaweed forests are rapidly changing with climate impacts and other human stressors throughout much of their range⁴⁷, with losses in many regions outpacing actions to restore these ecosystems⁴⁸ but with seaweed forests expanding in some warming polar regions^{49,50}. Quantifying the consequences of shifts in seaweed forest distribution and abundance on coastal carbon budgets can generate impetus for their protection and restoration and provide essential information on CO₂ emissions from past losses. The role of seaweed forests in cycling and storing carbon is currently not included in estimates of carbon sequestration, and this omission risks underestimating the consequences of losing these ecosystems and the benefits of their protection and restoration.

Online content

Any methods, additional references, Nature Portfolio reporting summaries, source data, extended data, supplementary information, acknowledgements, peer review information; details of author contributions and competing interests; and statements of data and code availability are available at <https://doi.org/10.1038/s41561-024-01449-7>.

References

- Boyd, P. et al. Multi-faceted particle pumps drive carbon sequestration in the ocean. *Nature* **568**, 327–335 (2019).
- Henson, S. A. et al. Uncertain response of ocean biological carbon export in a changing world. *Nat. Geosci.* <https://doi.org/10.1038/s41561-022-00927-0> (2022)
- Duarte, C. M., Gattuso, J., Hancke, K., Gundersen, H. & Filbee-Dexter, K. Global estimates of the extent and production of macroalgal forests. *Glob. Ecol. Biogeogr.* **31**, 1422–1439 (2022).
- Pessarrodona, A. et al. Global seaweed productivity. *Sci. Adv.* **8**, 2465 (2022).
- Watanabe, K. et al. Macroalgal metabolism and lateral carbon flows can create significant carbon sinks. *Biogeosciences* **17**, 2425–2440 (2020).
- Weigel, B. L. & Pfister, C. A. The dynamics and stoichiometry of dissolved organic carbon release by kelp. *Ecology* **102**, e03221 (2021).
- Krumhansl, K. & Scheibling, R. Production and fate of kelp detritus. *Mar. Ecol. Prog. Ser.* **467**, 281–302 (2012).
- Filbee-Dexter, K., Wernberg, T., Ramirez-Llodra, E., Norderhaug, K. M. & Pedersen, M. F. Movement of pulsed resource subsidies from shallow kelp forests to deep fjords. *Oecologia* **187**, 291–304 (2018).
- Fram, J. P. et al. Physical pathways and utilization of nitrate supply to the giant kelp, *Macrocystis pyrifera*. *Limnol. Oceanogr.* **53**, 1589–1603 (2008).
- Vetter, E. W. & Dayton, P. K. Macrofaunal communities within and adjacent to a detritus-rich submarine canyon system. *Deep Sea Res.* **2** **45**, 25–54 (1998).

11. Krause-Jensen, D. & Duarte, C. M. Substantial role of macroalgae in marine carbon sequestration. *Nat. Geosci.* **9**, 737–742 (2016).
12. Queiros, A. M. et al. Connected macroalgal–sediment systems: blue carbon and food webs in the deep coastal ocean. *Ecol. Monogr.* **89**, e01366 (2019).
13. Pessarrodona, A. et al. Carbon sequestration and climate change mitigation using macroalgae: a state of knowledge review. *Biol. Rev.* <https://doi.org/10.1111/brv.12990> (2023).
14. Ortega, A. et al. Important contribution of macroalgae to oceanic carbon sequestration. *Nat. Geosci.* **12**, 748–754 (2019).
15. Hurd, C. L. et al. Forensic carbon accounting: assessing the role of seaweeds for carbon sequestration. *J. Phycol.* **58**, 347–363 (2022).
16. Macreadie, P. I. et al. Operationalizing marketable blue carbon. *One Earth* **5**, 485–492 (2022).
17. Filbee-Dexter, K. & Wernberg, T. Substantial blue carbon in overlooked Australian kelp forests. *Sci. Rep.* **10**, 12341 (2020).
18. Ager, T. G. et al. Macroalgal habitats support a sustained flux of floating biomass but limited carbon export beyond a Greenland fjord. *Sci. Total Environ.* **872**, 162224 (2023).
19. Queirós, A. M. et al. Identifying and protecting macroalgae detritus sinks toward climate change mitigation. *Ecol. Appl.* <https://doi.org/10.1002/EAP.2798> (2022).
20. Vanderklift, M. A. et al. A guide to international climate mitigation policy and finance frameworks relevant to the protection and restoration of blue carbon ecosystems. *Front. Mar. Sci.* <https://doi.org/10.3389/fmars.2022.872064> (2022).
21. Broch, O. J., Hancke, K. & Ellingsen, I. H. Dispersal and deposition of detritus from kelp cultivation. *Front Mar. Sci.* **9**, 840531 (2022).
22. Filbee-Dexter, K. et al. Kelp carbon sink potential decreases with warming due to accelerating decomposition. *PLoS Biol.* **20**, e3001702 (2022).
23. Harrold, C. & Lisin, S. Radio-tracking rafts of giant kelp: local production and regional transport. *J. Exp. Mar. Biol. Ecol.* **130**, 237–251 (1989).
24. Dai, M. et al. Carbon fluxes in the coastal ocean: synthesis, boundary processes, and future trends. *Ann. Rev. Earth Planet. Sci.* **50**, 593–626 (2022).
25. Hofmann, E. E. et al. Modeling the dynamics of continental shelf carbon. *Ann. Rev. Mar. Sci.* **3**, 93–122 (2011).
26. Pedersen, M., Filbee-Dexter, K., Frisk, N., Sárossy, Z. & Wernberg, T. Carbon sequestration potential increased by incomplete anaerobic decomposition of kelp detritus. *Mar. Ecol. Prog. Ser.* <https://doi.org/10.3354/meps13613> (2021).
27. Trevathan-Tackett, S. M. et al. Comparison of marine macrophytes for their contributions to blue carbon sequestration. *Ecology* **96**, 3043–3057 (2015).
28. Queirós, A. M. et al. Connected macroalgal–sediment systems: blue carbon and food webs in the deep coastal ocean. *Ecol. Monogr.* <https://doi.org/10.1002/ecm.1366> (2019).
29. Frigstad, H. et al. *Blue Carbon—Climate Adaptation, CO₂ Uptake and Sequestration of Carbon in Nordic Blue Forests* (Nordic Council of Ministers, 2021); <https://doi.org/10.6027/temanord2020-541>
30. Allen, S. E. & Durrieu de Madron, X. A review of the role of submarine canyons in deep-ocean exchange with the shelf. *Ocean Sci.* **5**, 607–620 (2009).
31. Siegel, D. A., DeVries, T., Doney, S. C. & Bell, T. Assessing the sequestration time scales of some ocean-based carbon dioxide reduction strategies. *Environ. Res. Lett.* **16**, 104003 (2021).
32. Fragkopoulou, E. et al. Global biodiversity patterns of marine forests of brown macroalgae. *Glob. Ecol. Biogeogr.* **31**, 636–648 (2022).
33. Liu, X. et al. Simulating water residence time in the coastal ocean: a global perspective. *Geophys. Res. Lett.* **46**, 13910–13919 (2019).
34. Nowicki, M., DeVries, T. & Siegel, D. A. Quantifying the carbon export and sequestration pathways of the ocean’s biological carbon pump. *Glob. Biogeochem. Cycles* **36**, e2021GB007083 (2022).
35. Friedlingstein, P. et al. Global carbon budget. *Earth Syst. Sci. Data* **14**, 1917–2005 (2022).
36. De La Rocha, C. L. & Passow, U. in *Treatise on Geochemistry* 2nd edn, Vol. 8 (eds Holland, H. D. & Turekian, K. K.) 93–122 (Elsevier, 2014).
37. Hernández-León, S. et al. Large deep-sea zooplankton biomass mirrors primary production in the global ocean. *Nat. Commun.* **11**, 11 (2020).
38. Cooley, S. et al. in *IPCC Climate Change 2022: Impacts, Adaptation and Vulnerability* (eds Pörtner, H.-O. et al) Ch. 3 (Cambridge Univ. Press, 2022).
39. Smith, S. V. Marine macrophytes as a global carbon sink. *Science* **211**, 838–840 (1981).
40. Arndt, S. et al. Quantifying the degradation of organic matter in marine sediments: a review and synthesis. *Earth Sci. Rev.* **123**, 53–86 (2013).
41. Smith, R. W., Bianchi, T. S., Allison, M., Savage, C. & Galy, V. High rates of organic carbon burial in fjord sediments globally. *Nat. Geosci.* **8**, 450–453 (2015).
42. Macreadie, P. I. et al. The future of blue carbon science. *Nat. Commun.* **10**, 3998 (2019).
43. Buck-Wiese, H. et al. Fucoid brown algae inject fucoidan carbon into the ocean. *Proc. Natl Acad. Sci. USA* **120**, 2210561119 (2023).
44. Li, H. et al. Carbon sequestration in the form of recalcitrant dissolved organic carbon in a seaweed (kelp) farming environment. *Environ. Sci. Technol.* **56**, 9112–9122 (2022).
45. Paine, E. R., Schmid, M., Boyd, P. W., Diaz-Pulido, G. & Hurd, C. L. Rate and fate of dissolved organic carbon release by seaweeds: a missing link in the coastal ocean carbon cycle. *J. Phycol.* <https://doi.org/10.1111/jpy.13198> (2021).
46. van der Mheen, M. et al. Substantial kelp detritus exported beyond the continental shelf by dense shelf water transport. *Sci. Rep.* **14**, 839 (2024).
47. Wernberg, T., Krumhansl, K. A., Filbee-Dexter, K. & Pedersen, M. F. in *World Seas: An Environmental Evaluation* 2nd edn, Vol. 3 (ed. Sheppard, C.) 57–78 (Academic Press, 2019).
48. Filbee-Dexter, K. et al. Leveraging the blue economy to transform marine forest restoration. *J. Phycol.* **58**, 198–207 (2022).
49. Krause-Jensen, D. et al. Imprint of climate change on pan-Arctic marine vegetation. *Front. Mar. Sci.* **7**, 617324 (2020).
50. Amsler, C. D. et al. Strong correlations of sea ice cover with macroalgal cover along the Antarctic Peninsula: ramifications for present and future benthic communities. *Elementa* **11**, 00020 (2023).

Publisher’s note Springer Nature remains neutral with regard to jurisdictional claims in published maps and institutional affiliations.

Springer Nature or its licensor (e.g. a society or other partner) holds exclusive rights to this article under a publishing agreement with the author(s) or other rightsholder(s); author self-archiving of the accepted manuscript version of this article is solely governed by the terms of such publishing agreement and applicable law.

© The Author(s), under exclusive licence to Springer Nature Limited 2024

¹Institute of Marine Research, His, Norway. ²School of Biological Sciences and Oceans Institute, University of Western Australia, Perth, Western Australia, Australia. ³International Blue Carbon Institute, Singapore, Singapore. ⁴Department of Science and Environment, Roskilde University, Roskilde, Denmark. ⁵Red Sea Research Center (RSRC) and Computational Bioscience Research Center (CBRC), King Abdullah University of Science and Technology (KAUST), Thuwal, Kingdom of Saudi Arabia. ⁶Centre of Marine Sciences, University of the Algarve, Faro, Portugal. ⁷Faculty of Bioscience and Aquaculture, Nord University, Bodø, Norway. ⁸Norwegian Institute for Water Research (NIVA), Oslo, Norway. ⁹Scottish Association for Marine Science, Oban, UK. ¹⁰Optical Oceanography, Institute of Carbon Cycles, Helmholtz-Zentrum Hereon, Geesthacht, Germany. ¹¹Radar Hydrography, Institute of Coastal Ocean Dynamics, Helmholtz-Zentrum Hereon, Geesthacht, Germany. ¹²Laboratoire d'Océanographie de Villefranche, Sorbonne Université, CNRS, Villefranche-sur-Mer, France. ¹³Institute for Sustainable Development and International Relations, Paris, France. ¹⁴Fisheries and Oceans Canada, Bedford Institute of Oceanography, Dartmouth, Nova Scotia, Canada. ¹⁵Coastal and Estuarine Environment Research Group, Port and Airport Research Institute, Yokosuka, Japan. ¹⁶Department of Earth Sciences, Utrecht University, Utrecht, the Netherlands. ¹⁷Dove Marine Laboratory, School of Natural and Environmental Sciences, Newcastle University, Newcastle-upon-Tyne, UK. ¹⁸Plymouth Marine Laboratory, Plymouth, UK. ¹⁹Marine Biological Association of the United Kingdom, Citadel Hill, Plymouth, UK. ²⁰Ciimar and Faculty of Sciences, University of Porto, Porto, Portugal. ²¹Institute of Coastal Ocean Dynamics, Helmholtz-Zentrum Hereon, Geesthacht, Germany. ²²Aarhus University, Department of Ecoscience, Aarhus, Denmark.

✉ e-mail: kfilbeedexter@gmail.com

Methods

We used models of the primary production of seaweed forests, maps of their global distribution, estimates of detritus longevity and estimates of coastal residence time from ocean hydrographic models to estimate the amount of seaweed POC exported beyond the continental shelf globally. Our approach combined several state-of-the-art models publicly available to the oceanographic community with de novo compilations of seaweed decomposition rates and detritus transport characteristics. We limited our analyses to canopy-forming brown seaweed of the orders Desmarestiales, Fucales, Laminariales and Tilopteridales because there was more information on their productivity⁴ and area³² and because these seaweed forests are the focus of attention for carbon mitigation potential.

Seaweed area

We obtained the global estimates of the distribution of brown seaweed forests from published species distribution models (420 species in total; 36 intertidal and 384 subtidal), which were bounded by 30 m depth and at a 0.5° spatial resolution³². The distribution of seaweed forests was derived from a dataset of 2.8 million records of seaweeds sourced from herbaria, literature and data repositories³¹, with gaps in distributions filled using the environmental niche where records occurred³². The seaweed distribution models were developed using long-term average environmental predictors from between 2000 and 2017 of temperature, light, nutrients, sea ice, salinity and wave energy³². We included only attached seaweed and excluded all holopelagic seaweed (for example *Sargassum fluitans* and *S. natans*). We classified attached species into two categories of transportation after detachment: floating species, with gas-filled vesicles or tissues that keep them on the ocean surface after detachment, and sinking species, which are negatively buoyant. We determined the areal extent of both categories of seaweeds using these distribution models (Supplementary Information and Supplementary Data 1).

Productivity

Area-specific estimates of the amount of carbon fixed by seaweed forests were obtained from a published subtidal global model of NPP⁴, which used a dataset of 659 records from 151 independent studies published between 1967 and 2019. This captured in situ measurements across a range of depths at 277 independent sites and from 128 forest-forming taxa. To correct for high values in the NPP model, which appeared mainly in regions with little to no data inputs, we constrained all NPP values to the 95th quantile (1,684 gC m⁻²y⁻¹), which is below the maxima measured in the wild⁵².

Decomposition

The amount of remaining seaweed biomass available for potential sequestration, for example, in deep ocean sinks, depends on the decay rate, which can be affected by an interplay of abiotic factors (for example, temperature, UV radiation, water motion and oxygen levels) as well as biotic factors (grazing, microbial communities, growth, epiphytes, decomposition and tissue composition)^{26,27,53}. To determine residence times of seaweeds in the coastal zone, we used a global dataset compiled de novo from decomposition measures from laboratory and in situ experiments of seaweed biomass or carbon loss over time, for Desmarestiales, Fucales, Laminariales and Tilopteridales (Extended Data Fig. 1). We converted biomass to carbon using species-specific conversion ratios where possible⁴. We found no consistent taxon-specific (for example, family level) and geographically specific (national and/or state level and ecoregion level⁵⁴) relationship with decomposition rates that would enable us to model decomposition across the global distribution of these orders of seaweeds. We did not account for environmental drivers of decomposition rates, such as temperature, that may affect the longevity of transported carbon, spatially and temporally²², because temperature–decomposition relationships remain poorly resolved for most seaweed species.

Export below 200 m depth

We calculated the per area potential export of seaweed carbon to deep marine sinks (gC m⁻² y⁻¹) using different formulas for sinking and floating species. For sinking seaweed species, export was calculated as:

$$\text{Export.S} = e^{-\text{CRT} \times k} \times 0.71$$

Where 0.71 is the proportion of NPP that entered the water column as detritus (Supplementary Information), CRT is the coastal residence time and k is the decomposition rate.

CRT was defined as the elapsed time in days for a parcel of source water in the coastal domain to exit to the open ocean (beyond the 200 m isobath) and was calculated for the distribution of seaweed forests using the National Oceanic and Atmospheric Administration Modular Ocean Model, the highest available resolution global current model⁵⁵, which tracked parcels of coastal water bodies in three dimensions at 0.125° resolution and then calculated an average CRT for each starting point from 1998 to 2007³³. We retained the higher resolution of the CRT models (0.125° compared with 0.5° for the NPP and global distribution models) to ensure that the full range of export was included in our estimates and refer to these as the ‘coastal cells’. At this resolution, the CRT model probably only partially captures meso-scale processes such as offshore winds, riverine flows or dense shelf-water transport, which can create offshore currents and increase export⁵⁶. We cropped these CRT models to the coastline using 50 m depth cut-off (Bio-ORACLE, maximum depth bathymetry layer). The lower growth limit of seaweed can extend beyond 200 m, but most occur shallower than 30 m depth⁴⁷ and seaweed detritus is abundant at 0–50 m depths^{57–59}.

For floating species, we collated studies on the average floating longevity (FL) for seaweeds to estimate the number of days seaweed detritus would be transported in surface currents before it became negatively buoyant (average from studies in natural settings 31.7 days, 9.1 SE, $n = 9$; Supplementary Data 1). For cells where floating longevity was shorter than the CRT, we used the same calculation for the sinking species, which assumed that floating seaweeds that sink before they cross 200 m depth are transported as bedload. However, for cells with floating longevity longer than CRT, we used the floating longevity to estimate the percentage seaweed carbon remaining when the seaweed becomes negatively buoyant and sinks to deep regions.

$$\text{Export.F} = e^{-\text{FL} \times \text{CRT} \times k} \times 0.71$$

This approach is conservative as it does not account for fragmentation of sinking particles or continued production during surface transport in waters deeper than 200 m depth⁶⁰.

For sinking species, we calculated an average deposition time of POC to 200 m depth of 1.3 hours (range of 20 minutes to 7 hours), on the basis of published in situ measures of sinking speeds for brown seaweeds (Supplementary Data 1). Given that CRTs were longer (days) than this deposition time, we assumed all sinking seaweed were transported along the seafloor, and some reached beyond the shelf break and eventually sank to the deeper ocean. We classified all coastal cells containing seaweed forests into two categories, bedload transport or bedload retention, using minimum threshold bottom current speeds (0.045 m s⁻¹ ± 0.004 SE) measured using flume experiments (Supplementary Data 1), which enable the passive movement of seaweeds along the seafloor for the four orders. For floating species, we classified areas as bedload retention where FL < CRT and bottom current speeds were <0.045 m s⁻¹, and where FL > CRT we assumed no bedload retention occurred. In total, 88% of all modelled coastal raster cells within the distribution of seaweed forests had seafloor currents fast enough to transport sinking seaweed detritus as bedload in any direction.

It was not possible to determine the relative abundance of floating and sinking seaweed for each seaweed forests cell using the presence/absence species distribution models. Therefore, for coastal cells with

combined floating and sinking species (46% of total), we used the average of percentage export of floating and sinking seaweeds for that cell to estimate export. For the coastal cells with floating seaweeds only (34% of total seaweed habitat) where $FL > CRT$, we estimated export using floating longevity, regardless of the velocity of the seafloor currents. Coastal areas with negatively buoyant seaweed only (20% of total) that did not satisfy experimentally determined water movement thresholds for seaweed bedload transport were assigned an export rate of 0%.

The export was calculated using the available time for detritus to be transported (CRT or FL), on the basis of seaweed decomposition rates, for each cell in our seaweed forest distribution model. To capture the range of decomposition rates for brown seaweed detritus, we used a weighted quantile estimate of k values for ten quantiles in the global dataset of decomposition. This ensured that seaweed tissue components that decompose slowly were included in our estimates as this material has the highest likelihood of export²⁶ and could be underestimated or excluded by taking a median k value. We selected only ten quantiles to exclude the upper and lower 5% of these decomposition rates to ensure calculations were not influenced by outlier data. To assess the sensitivity of our analysis to variation in decomposition rates (which exist over differences in geography and taxa^{22,53}), we compared this weighted quantile estimate with estimates calculated using the slowest (bottom 25%) and fastest (top 25%) of these decomposition quantiles (Supplementary Information).

To calculate total seaweed carbon export (gC yr^{-1}) beyond the 200 m depth shelf break for each geopolitical and ecological relevant area, we estimated the average per area annual production ($\text{gC m}^{-2} \text{yr}^{-1}$) (ref. 4) and export of seaweed POC for each ecoregion⁵⁴ and national EEZ. Because seaweed distribution models did not include percentage rocky substrata, we corrected national EEZ area estimates using national estimates for percentage rock along the coastline⁶¹. We corrected all ecoregion area estimates using 46% rock, on the basis of the average national percentage rock estimates⁶¹, weighted by seaweed area within EEZs. This difference in the percentage rock correction resulted in higher total seaweed carbon export estimates across all ecoregions compared with all EEZs. However, as the percentage rock corrections were more precise for EEZs compared with ecoregions, we used EEZ areas to determine total carbon export and estimates of sequestration. We estimated upper and lower ranges for the export of seaweed POC for each EEZ and ecoregion using the slowest and fastest estimates for decomposition rates (see the preceding) and the 25% and 75% quantiles percentage NPP released as detritus (Supplementary Information).

Seaweed export through 200 m was compared with global estimates of the biological pump (10.2 GtC yr^{-1} (ref. 34)) and carbon uptake in the global ocean CO_2 sink (2.8 GtC yr^{-1} (ref. 35)), which is estimated using export beyond 100 m depth. To enable a direct comparison, we adjusted these estimates to 200 m using the Martin's equation for carbon flux⁶², using a range of global b exponents of -0.70 to -0.98 (ref. 63), which aligns with other b exponent ranges reported for these depths^{64,65}.

$$C_{\text{flux}} = F_0 \left(\frac{z}{100} \right)^b$$

This correction resulted in a global estimate of the biological pump export at 200 m of 5.2 – 6.3 GtC yr^{-1} and global ocean CO_2 sink of 1.4 – 1.7 GtC yr^{-1} . We also compared our estimates for seaweed forests with estimates of total carbon sequestration by three other blue carbon ecosystems: salt marshes (12.6 TgC yr^{-1}), mangrove forests (41.0 TgC yr^{-1}) and seagrass meadows (35.3 TgC yr^{-1})³⁸.

Several sources of variation were not captured with our approach of using a global current model of coastal water bodies to estimate seaweed carbon transport. Wind and waves can be an important driver of transport for floating seaweed, whose drifting trajectories vary depending on the prevailing winds at the time of release^{18,66}. The

hydrographic model we used (the National Oceanic and Atmospheric Administration Modular Ocean Model⁵⁵) does not include tides, which have important effects on nearshore currents and export of seaweed¹⁸, as well as POC resuspension due to the tidally induced turbulence near the seafloor, so these models probably poorly capture export in areas with strong tidal influence (for example, United Kingdom, eastern Canada, Greenland, Gulf of Maine, Argentina, northwest Australia and eastern Russia). We assumed passive seaweed transport with a large-sized coastal water mass (0.125° resolution), but the actual transport may be influenced by numerous fine-scale local factors, such as reef topography⁵⁹, basins or skerries that trap detritus^{18,58}, local variation in site exposure²¹ and sub-grid-scale processes, such as eddies⁶⁷. Large seaweed fragments (for example, entire plants or rafts) are probably impacted by inertial effects⁶⁸. Yet most of the detritus is composed by smaller fragments and particulate carbon produced by erosion^{69,70}, for which passive transport probably approximates their movement within the water column⁷¹. Bottom type may also impact resuspension and bedload movement⁷². Furthermore, the coastal residence time estimates do not resolve small-scale (sub-meso-scale and smaller) ocean processes that strongly impact the transport and dispersion of tracers such as DOC and POC⁷³ and are not specific to the bottom waters where negatively buoyant POC are transported, but instead integrate the full water column.

Sequestration timescales for exported seaweed carbon

We estimated the time it would take seaweed carbon that was remineralized at 200 and 530 m depths to return to the sea surface where it could reenter the atmosphere using published models of the fraction of injected CO_2 in the deep ocean that remains sequestered over time³¹. These were based on an ocean circulation inverse model, which is a steady-state global ocean transport model with a horizontal resolution of 2° and 48 vertical levels⁷⁴. We selected 200 and 530 m depths because they were reported by ref. 31 and were the most relevant for our POC export estimates beyond 200 m depth. We also report 1,000 m depth for ecoregions where these depths occur close to the shelf break ($n = 117$) as this is a sequestration depth horizon traditionally presented for seaweed carbon¹¹. Using these modelled sequestration timescales, we calculated the median sequestration time in years and the median fraction of discharged carbon that remains sequestered for 25 and 100 years at 200, 530 and 1,000 m depths for each ecoregion⁵⁴ within the distribution of seaweed forests. For these calculations, we used a k -nearest neighbour ($k = 1$) to determine the nearest sequestration time and sequestration fraction within 10° maximum grid of each coastal cell (0.125° resolution) within the distribution of seaweed forests. To determine the total amount of seaweed carbon reaching deep areas with different timescales of sequestration, we weighted our modelled estimates of median sequestration time for each ecoregion by the total seaweed carbon exported beyond the shelf for each ecoregion. We summed these estimates to calculate the cumulative seaweed carbon reaching a range of sequestration timescales (from 0 to 230 years) globally. We used measures of sequestration fractions to calculate the median sequestration fraction at 25 and 100 years for each ecoregion, as well as the range across biogeographic realm⁵⁴. To estimate the amount of seaweed carbon potentially sequestered for 25 and 100 years at 200 and 530 m depths, we used two approaches. First, we summed the total seaweed exported from ecoregions with median sequestration timescales greater than 25 or 100 years for both depths. Second, we summed the product of the total seaweed export (TgC) and the sequestration fraction at 25 and 100 years for both depths and across all ecoregions. This produced an upper and lower estimate for different depths and timescales.

We performed all analyses using R 4.2.2 (ref. 78).

Data availability

Data for national and ecoregion area estimates, percentage export, carbon export, NPP, decomposition and other parameters are available in

Supplementary Data 1. Additional information on uncertainties around parameters and assumptions are provided in Supplementary Information. Predictive layers and model outputs of CRT, percentage export data and POC export are available at figshare (<https://doi.org/10.6084/m9.figshare.24116973>) (ref. 77). Areal estimates for floating and sinking seaweed forest were modelled from species occurrence records⁵¹ and stacked distribution estimates³² that are openly available at figshare (<https://doi.org/10.6084/m9.figshare.14496018.v4>) (ref. 75). Benthic currents and bathymetric data are available from Bio-ORACLE⁷⁶. Source data for net primary productivity models are openly available⁴, and the dataset is described in Scientific Data (<https://doi.org/10.1038/s41597-022-01554-5>). Source CRTs³³ are archived at NOAA GFDL (ftp://data1.gfdl.noaa.gov/users/Xiao.Liu/CRT_simulation/GFDL-MOM6-SIS2/).

Code availability

Source code is available at figshare (<https://doi.org/10.6084/m9.figshare.24116973>)⁷⁷.

References

- Assis, J. et al. A fine-tuned global distribution dataset of marine forests. *Sci. Data* **7**, 119 (2020).
- Fairhead, V. A. *Ecophysiology and Production Ecology of the Kelp Ecklonia radiata (C. Agardh) J. Agardh, at West Island, South Australia*. PhD thesis, Univ. Adelaide (2001).
- Wright, L. S., Pessarrodona, A. & Foggo, A. Climate-driven shifts in kelp forest composition reduce carbon sequestration potential. *Glob. Change Biol.* **28**, 5514–5531 (2022).
- Spalding, M. D. et al. Marine ecoregions of the world: a bioregionalization of coastal and shelf areas. *Bioscience* **57**, 573–583 (2007).
- Griffies, S. M., Adcroft, A. & Hallberg, R. A primer on the vertical Lagrangian-remap method in ocean models based on finite volume generalized vertical coordinates. *J. Adv. Model. Earth Syst.* **12**, 10 (2020).
- Mahjabin, T., Pattiaratchi, C. & Hetzel, Y. Occurrence and seasonal variability of Dense Shelf Water Cascades along Australian continental shelves. *Sci. Rep.* **10**, 9732 (2020).
- Smale, D. A., Pessarrodona, A., King, N. & Moore, P. J. Examining the production, export, and immediate fate of kelp detritus on open-coast subtidal reefs in the Northeast Atlantic. *Limnol. Oceanogr.* **67**, S36–S49 (2022).
- Filbee-Dexter, K. & Scheibling, R. E. Spatial patterns and predictors of drift algal subsidy in deep subtidal environments. *Estuaries Coasts* **39**, 1724–1734 (2016).
- Britton-Simmons, K. H. et al. Habitat and bathymetry influence the landscape-scale distribution and abundance of drift macrophytes and associated invertebrates. *Limnol. Oceanogr.* **57**, 176–184 (2012).
- Frontier, N., de Bettignies, F., Foggo, A. & Davoult, D. Sustained productivity and respiration of degrading kelp detritus in the shallow benthos: detached or broken, but not dead. *Mar. Environ. Res.* **166**, 105277 (2021).
- Young, A. P. & Carilli, J. E. Global distribution of coastal cliffs. *Earth Surf. Process. Landf.* **44**, 1309–1316 (2019).
- Martin, J. H., Knauer, G. A., Karl, D. M. & Broenkow, W. W. VERTEX: carbon cycling in the northeast Pacific. *Deep Sea Res. A* **34**, 267–285 (1987).
- Lauderdale, J. M. & Cael, B. B. Impact of remineralization profile shape on the air–sea carbon balance. *Geophys. Res. Lett.* **48**, e2020GL091746 (2021).
- Guidi, L. et al. A new look at ocean carbon remineralization for estimating deepwater sequestration. *Glob. Biogeochem. Cycles* **29**, 1044–1059 (2015).
- Buesseler, K. O. & Boyd, P. W. Shedding light on processes that control particle export and flux attenuation in the twilight zone of the open ocean. *Limnol. Oceanogr.* **54**, 1210–1232 (2009).
- Hobday, A. J. Abundance and dispersal of drifting kelp *Macrocystis pyrifera* rafts in the Southern California Bight. *Mar. Ecol. Prog. Ser.* **195**, 101–116 (2000).
- Barnier, B., Penduff, T. & Langlais, C. in *Operational Oceanography in the 21st Century* (eds Schiller, A. & Brassington, G. B.) 239–262 (Springer, 2011).
- Olascoaga, M. J., Beron-Vera, F. J. & Miron, P. Observation and quantification of inertial effects on the drift of floating objects at the ocean surface. *Phys. Fluids* **32**, 26601 (2020).
- Krumhansl, K. & Scheibling, R. Detrital production in Nova Scotian kelp beds: patterns and processes. *Mar. Ecol. Prog. Ser.* **421**, 67–82 (2011).
- Pedersen, M. F. et al. Detrital carbon production and export in high latitude kelp forests. *Oecologia* **192**, 227–239 (2020).
- Wernberg, T. & Filbee-Dexter, K. Grazers extend blue carbon transfer by slowing sinking speeds of kelp detritus. *Sci. Rep.* **8**, 17180 (2018).
- Carvajalino-Fernández, M. A., Sævik, P. N., Johnsen, I. A., Albretsen, J. & Keeley, N. B. Simulating particle organic matter dispersal beneath Atlantic salmon fish farms using different resuspension approaches. *Mar. Pollut. Bull.* **161**, 111685 (2020).
- D’Asaro, E. A. et al. Ocean convergence and the dispersion of flotsam. *Proc. Natl Acad. Sci. USA* **115**, 1162–1167 (2018).
- Holzer, M., DeVries, T. & de Lavergne, C. Diffusion controls the ventilation of a Pacific Shadow Zone above abyssal overturning. *Nat. Commun.* **12**, 4348 (2021).
- Fragkopoulou, E. et al. Global diversity patterns of marine forests of brown microalgae. *figshare* <https://doi.org/10.6084/m9.figshare.14496018.v4> (2021).
- Assis, J. et al. Bio-ORACLE v2.0: extending marine data layers for bioclimatic modelling. *Glob. Ecol. Biogeogr.* **27**, 277–284 (2018).
- Filbee-Dexter, K. et al. Carbon export from seaweed forests to deep ocean sinks. *figshare* <https://doi.org/10.6084/m9.figshare.24116973> (2024).
- R Core Team. R: A language and environment for statistical computing. <https://www.R-project.org/> (R Foundation for Statistical Computing, 2021).

Acknowledgements

This work was supported by the Norwegian Blue Forest Network and EUROMARINE (FWS_07-2018). The project was funded by the Australian Research Council (DE190100692, FT230100214, DP220100650, LP220200004) to K.F.-D., T.W. and A.P., the Independent Research Fund Denmark (8021-00222 B, ‘CARMA’) to D.K.-J., and the Foundation for Science and Technology (UIDB/04326/2020, UIDP/04326/2020, LA/P/0101/2020) and Individual Call to Scientific Employment Stimulus (2022.00861.CEECIND/CP1729/CT0003) to J.A. Flume experiments used for benthic transport were conducted in collaboration with A. Pomeroy.

Author contributions

K.F.-D., A.P., M.F.P., T.W., C.M.D., J.A., T.B., M.T.B., D.F.C., J.-P.G., H.G., K.H., K.A.K., T.K., J.J.M., P.J.M., A.M.Q., D.A.S., I.S.P., N.S. and D.K.-J. conceptualized this study over two workshops, one led by D.K.-J. and C.M.D. and one led by K.F.-D. K.F.-D. ran the simulations, analysed the data and wrote the original draft of the manuscript, with contributions from A.P., M.F.P., T.W. and D.K.-J. The seaweed forest area distributions were calculated by J. A., the data on percentage net primary production exported as detrital materials were compiled by A.P. and K.A.K., and the decomposition rates were compiled by M.F.P. A.P., M.F.P., T.W., C.M.D., J.A., T.B., M.T.B., D.F.C., J.-P.G., H.G., K.H., K.A.K., T.K., J.J.M., P.J.M., A.M.Q., D.A.S., I.S.P., N.S. and D.K.-J. provided inputs to the writing and comments on the final draft.

Competing interests

The authors declare no competing interests.

Additional information

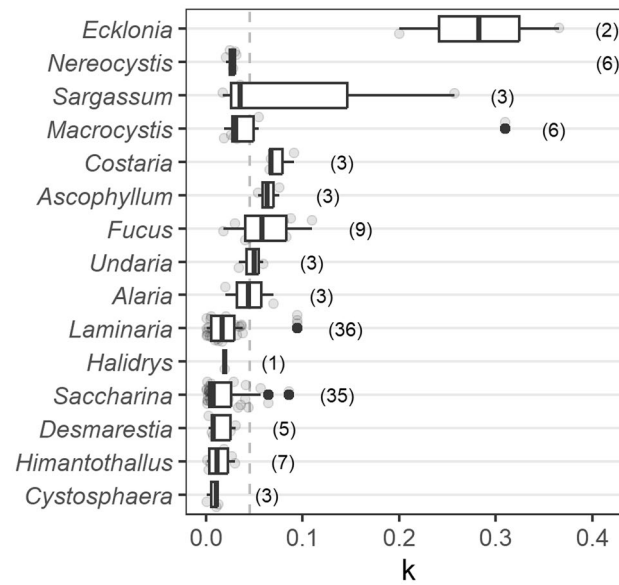
Extended data is available for this paper at <https://doi.org/10.1038/s41561-024-01449-7>.

Supplementary information The online version contains supplementary material available at <https://doi.org/10.1038/s41561-024-01449-7>.

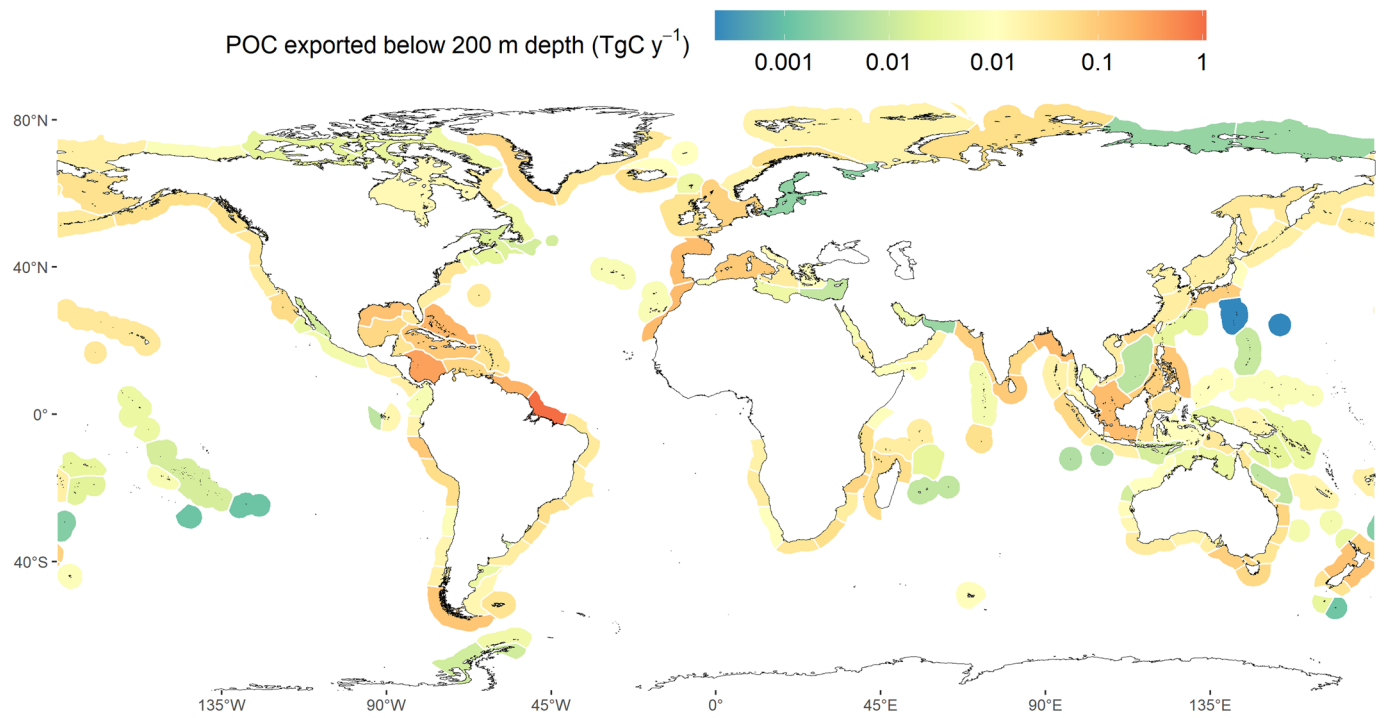
Correspondence and requests for materials should be addressed to Karen Filbee-Dexter.

Peer review information *Nature Geoscience* thanks Alecia Bellgrove, Charlotte Laufkötter, Matthias Schmid and the other, anonymous, reviewer(s) for their contribution to the peer review of this work. Primary Handling Editor: James Super, in collaboration with the *Nature Geoscience* team.

Reprints and permissions information is available at www.nature.com/reprints.



Extended Data Fig. 1 | Seaweed carbon decomposition. Range of decomposition rates (k) for brown seaweed genera. Dashed line shows global mean. Boxplots show the median and 25th and 75th percentiles and whiskers show 1.5 the inter-quartile range. Number of data points are shown in brackets. One outlier value for *Nereocystis* ($k = 1.33$) is not shown to aid visualization.



Extended Data Fig. 2 | Flux of seaweed carbon to deep ocean. Estimates of the total particulate organic carbon (POC) exported across the shelf and below 200-m depth in TgC y^{-1} for each ecoregion. Map shapefiles from Natural Earth.